Early fibrin biofilm development in cardiovascular infections

Oukrich, Safae; Hong, Jane; Leon-Grooters, Mariël; van Cappellen, Wiggert A.; Slotman, Johan A.; Koenderink, Gijsje H.; van Wamel, Willem J.B.; de Maat, Moniek P.M.; Kooiman, Klazina; Lattwein, Kirby R.

DOI
10.1016/j.bioflm.2025.100261

Publication date
2025

Document Version
Final published version

Published in
Biofilm

Biofilm 9 (2025) 100261

Contents lists available at ScienceDirect

Biofilm

journal homepage: www.sciencedirect.com/journal/biofilm

Early fibrin biofilm development in cardiovascular infections

Safae Oukrich [a,*], Jane Hong [a], Mariël Leon-Grooters [a], Wiggert A. van Cappellen [b], Johan A. Slotman [b], Gijsje H. Koenderink [c], Willem J.B. van Wamel [d], Moniek P.M. de Maat [e], Klazina Kooiman [a], Kirby R. Lattwein [a]

[a] Biomedical Engineering, Department of Cardiology, Cardiovascular Institute, Erasmus MC, P.O. Box 2040, 3000 CA, Rotterdam, the Netherlands
[b] Erasmus Optical Imaging Center, Erasmus MC, P.O. Box 2040, 3000 CA, Rotterdam, the Netherlands
[c] Department of Bionanoscience, Kavli Institute of Nanoscience, Delft University of Technology, P.O Box 5046, 2600 GA, Delft, the Netherlands
[d] Department of Medical Microbiology and Infectious Diseases, Erasmus MC, P.O. Box 2040, 3000 CA, Rotterdam, the Netherlands
[e] Department of Hematology, Cardiovascular Institute, Erasmus MC, P.O. Box 2040, 3000 CA, Rotterdam, the Netherlands

ARTICLE INFO

Keywords:
Biofilm development
Cardiovascular infections
Coagulase
Fibrin
Fibrinogen
Staphylococcus aureus

ABSTRACT

The single most common microbe causing cardiovascular infections is *Staphylococcus aureus* (*S. aureus*). *S. aureus* produces coagulase that converts fibrinogen to fibrin, which is incorporated into biofilms. This process aids in adherence to intravascular structures, defense against the host immune system, and resistance to antimicrobial treatment. Despite its significance, fibrin formation in *S. aureus* biofilms remains poorly understood. Therefore, this study aimed to elucidate the early development of cardiovascular biofilms. Clinically isolated coagulase-positive *S. aureus* and coagulase-negative *Staphylococcus lugdunensis* (*S. lugdunensis*) from patients with cardiovascular infections, and a coagulase mutant *S. aureus* Δcoa, were grown in tryptic soy broth (TSB), Iscove's Modified Dulbecco's Medium (IMDM), and pooled human plasma, with or without porcine heart valves. Bacterial growth, metabolic activity, and bacterial fibrinogen utilization were measured over 24 h at 37 °C. Time-lapse confocal microscopy was used to visualize and track biofilm development. *S. aureus* exhibited more growth in TSB and human plasma than *S. lugdunensis* and *S. aureus* Δcoa, but showed similar growth in IMDM after 24 h. Peak metabolic activity for all isolates was highest in TSB and lowest in human plasma. The presence of porcine valves caused strain-dependent alterations in time to peak metabolic activity. Confocal imaging revealed fibrin-based biofilm development exclusively in the coagulase-producing *S. aureus* strains. Between 2 and 6 h of biofilm development, 74.9 % ($p = 0.034$) of the fibrinogen from the medium was converted to fibrin. Variations in fibrin network porosity and density were observed among different coagulase-producing *S. aureus* strains. Fibrin formation is mediated by *S. aureus* coagulase and first strands occurred within 3 h for clinical strains after exposure to human plasma. This study stresses the importance of experimental design given the bacterial changes due to different media and substrates and provides insights into the early pathogenesis of *S. aureus* cardiovascular biofilms.

1. Introduction

Cardiovascular bacterial infections, such as infective endocarditis (IE), which occur within the heart, and infections involving indwelling cardiovascular devices, like pacemakers and left ventricular assist devices, are life threatening. IE has a 1-year mortality rate of up to 50 % [1], and cardiovascular device infections (CDI) have mortality rates ranging from 25 to 50 %, depending on the device [2–5]. The most common infecting bacterium is *S. aureus*, responsible for at least 28 % of IE and 54 % of CDI [1,6]. It is associated with prolonged hospital stays, higher mortality risk, and greater likelihood of surgical intervention needed to resolve the infection [7,8]. Standard treatment for IE and CDI involves intensive, prolonged antibiotic therapy, which is often ineffective because these are biofilm infections [9]. Bacteria within biofilms

This article is part of a special issue entitled: Eurobiofilms 2024 published in Biofilm.

* Corresponding author. Erasmus MC, Biomedical Engineering, Dept. of Cardiology, Office Ee2322, P.O. Box 2040, 3000 CA, Rotterdam, the Netherlands.
E-mail addresses: s.oukrich@erasmusmc.nl (S. Oukrich), j.hong@erasmusmc.nl (J. Hong), h.leonmorales-grooters@erasmusmc.nl (M. Leon-Grooters), w.vancappellen@erasmusmc.nl (W.A. van Cappellen), j.slotman@erasmusmc.nl (J.A. Slotman), g.h.koenderink@tudelft.nl (G.H. Koenderink), w.vanwamel@erasmusmc.nl (W.J.B. van Wamel), m.demaat@erasmusmc.nl (M.P.M. de Maat), k.kooiman@erasmusmc.nl (K. Kooiman), k.lattwein@erasmusmc.nl (K.R. Lattwein).

https://doi.org/10.1016/j.bioflm.2025.100261
Received 2 September 2024; Received in revised form 3 February 2025; Accepted 6 February 2025
Available online 7 February 2025

encase themselves in an extracellular matrix, which makes them at least 10 to 1000 times less susceptible to antibiotics than non-encased bacteria [10], and even 4000 times for cardiovascular-related biofilms [11]. Despite the important role that biofilms have on increasing treatment complexity and mortality, the mechanisms underlying their early formation within the cardiovascular system are still not well understood.

Cardiovascular infections are thought to arise from bacteria interacting with pre-existing damaged or inflamed endothelial cells or by adhering directly to devices [12]. It is widely hypothesized that the host coagulation is activated upon bacteria entering the bloodstream [6,13]. Staphylococci, streptococci, and enterococci cause at least 79 % of cardiovascular infections [6]. These bacteria all express proteins that bind fibrinogen, however, only staphylococci produce enzymes to also convert fibrinogen to fibrin [14–16]. *S. aureus* can induce coagulation via two coagulases, staphylocoagulase and von Willebrand factor binding protein (vWbp), which both can be surface-bound and secreted by bacteria. These coagulases bind directly to prothrombin, bypassing the standard host coagulation cascade, thereby inducing a conformation change and activating prothrombin, triggering the conversion of fibrinogen into fibrin [6,17]. Overall, little is known about the early formation and utilization of bacterial-induced fibrin in cardiovascular biofilms.

Human plasma is a more physiologically accurate growth medium to replicate cardiovascular biofilms compared to traditional bacterial or mammalian cell culture media, yet plasma alone is rarely utilized as a growth media. Commonly, studies have used varying concentrations of plasma supplemented with bacterial or mammalian cell culture media, such as up to 50 % plasma in Brain-Heart Infusion (BHI) [18], Mueller Hinton, and Tryptic Soy broth [19,20] 25 % or 30 % of plasma in 20 % or 70 % Roswell Park Memorial Institute medium (RPMI) [21], respectively. These studies demonstrated that the addition of plasma to the media enhances biofilm formation in a dose-dependent and isolate-dependent manner. For the few studies that used 100 % human plasma, calcium chloride was added with the planktonic bacterial inoculation to artificially rapidly induce clot polymerization [22,23]. In one study, fibrin biofilms have been grown on human-whole blood retracted clots in 100 % plasma without calcium chloride, with only 24 h end-point biofilm visualization being performed [24].

Here we aimed to understand the early development of fibrin biofilms in cardiovascular infections during the first 24 h of its formation. To first understand the impact of media choice and the substrate bacteria grow on, such as whether the infection occurs on heart tissue versus a hard surface (e.g. an indwelling device), we compared the bacterial growth and metabolic activity of clinical IE isolates of *S. aureus* and *Staphylococcus lugdunensis*, a coagulase negative species, along with a coagulase mutant *S. aureus* (*S. aureus* Δcoa), using three different growth media: Tryptic Soy broth (TSB), Iscove's Modified Dulbecco's Medium (IMDM), and 100 % human plasma. Fibrinogen utilization was measured during biofilm development and high-resolution fluorescence confocal microscopy was used to visualize biofilms grown in human plasma on porcine valves. Furthermore, time-lapse microscopy was used to track and analyze *S. aureus* fibrin formation in biofilms over time.

2. Materials and methods

2.1. Bacterial isolates

Staphylococcus aureus (*S. aureus*) 25268, *S. aureus* 50825, and *Staphylococcus lugdunensis* (*S. lugdunensis*) strains were isolated from patients diagnosed with IE at the Erasmus MC, the Netherlands and stored at −80 °C. According to institutional policy, bacterial isolates de-identified and anonymized are classified as non-human subject research and do not require informed consent. The coagulase mutant *S. aureus* strain (*S. aureus* Δcoa) was constructed from the widely-used wildtype lab strain 8325-4. *S. lugdunensis*, a coagulase-negative staphylococcal species, served as another control for *S. aureus* Δcoa. Before conducting experiments, *S. aureus* 25268, *S. aureus* 50825, *S. aureus* 8325–4 and *S. lugdunensis* were grown at 37 °C on 5 % sheep blood agar plates (tryptic soy agar; BD, Trypticase™, Thermo Fisher Scientific, Waltham, MA, USA). *S. aureus* Δcoa was grown on tryptic soy agar plates containing 5 μg/ml tetracycline. All strains were incubated overnight.

2.2. Biofilm formation

Biofilms were formed *in vitro* by suspending single bacterial colonies from overnight plate cultures in 4 ml of 0.9 % NaCl saline solution until an optical density (OD) of 0.5 (±0.05) was reached at 600 nm as determined using a cell density meter (Ultraspec 10, Amersham Biosciences, Little Chalfont, UK). The inoculated NaCl solution was added to growth medium to reach 10^6 colony forming units per ml. Biofilms were grown in either Tryptic Soy Broth (TSB), Iscove's Modified Dulbecco's Medium (IMDM; 11500556; Gibco, Bleiswijk, the Netherlands), or 100 % non-heat-inactivated human plasma (blood type O^+; pooled from 5 healthy donors and directly stored at −80 °C; anticoagulant citrate phosphate double dextrose; Sanquin, Rotterdam, the Netherlands). Before experiments, the growth medium was pre-warmed to 37 °C. Biofilms were cultured at 37 °C, with or without a 6 mm porcine valve punch biopsy in either sterile flat-bottom 96-well polystyrene tissue culture plates (CellStar; Greiner Bio-One, Alphen aan de Rijn, the Netherlands), CalWel inserts (SymCel, Solna, Sweden), 1.5 ml Eppendorf tubes, or tissue culture-treated μ-Slide mono-channels (80916; ibiTreat μ-Slide I0.8 Luer; Ibidi GmbH, Martinsried, Germany). Porcine hearts were acquired from a local butcher. The valve biopsies were excised, biopsied, and then pre-sterilized for 5 min in 0.25 % glutaraldehyde (11433488; glutaraldehyde, 25 % aqueous solution, Thermo Scientific Chemicals, Dublin, Ireland) and rinsed thoroughly. To investigate the influence of the substrate on biofilm development, porcine valve tissue was used to mimic native heart valve infections, while empty sample containers (wells, μ-Slides or inserts) were used to simulate non-native tissue infections. At least n = 3 was performed for all experiments.

2.3. Biofilm growth and microcalorimetry

Growth and metabolic activity over time was assessed for *S. aureus* 25268, *S. aureus* Δcoa, and *S. lugdunensis* using TSB, IMDM, and human plasma. For growth measurements, 200 μl of inoculated medium was added to each well of a the 96-well tissue culture plate. The plate was then placed in a microplate reader (FLUOstar Omega; BMG LABTECH GmbH, Orternberg, Germany) to measure growth (OD_{600}) every 15 min for 24 h at 37 °C. Microcalorimetry was used to assess the heat produced in microWatts (μW) over time to determine bacterial metabolic activity using the CalScreener (SymCel, Solna, Sweden), a closed and isothermal system. This method enables the measurement of metabolic activity in the presence of porcine valves, which is not feasible with optical density measurements. Inoculated media (200 μl) was added to CalWell inserts which were then placed in titanium cups (SymCel, Solna, Sweden) and loaded into the CalScreener for 24 h at 37 °C to determine heat flow over time.

2.4. Determination of bacterial fibrinogen utilization

Bacterial fibrinogen utilization was determined at 0, 1, 2, 3. 4, 6, 9, and 24 h using the functional Clauss method [25] on the Sysmex CS-5100 system (Siemens Healthineers, Den Haag, the Netherlands). Biofilms of *S. aureus* 25268, *S. aureus* 50825, *S. aureus* Δcoa, *S. aureus* 8325–4, and *S. lugdunensis* were grown in human plasma within Eppendorf tubes as described in section 2.2. Individual samples were prepared at each time point (n = 3) and centrifuged at 14,000 g for 10 min. The supernatant was then transferred to a new Eppendorf and centrifuged again at 15,000 g for 5 min and stored at −80 °C until measuring fibrinogen levels.

2.5. Bacteria and fibrin visualization

All images were acquired using a custom-built, upright Nikon A1R + confocal microscope [26]. Biofilms of *S. aureus* 25268, *S. aureus* Δcoa, *S. aureus* 8325–4 and *S. lugdunensis*, which were grown in human plasma on sterile porcine valve biopsies for 24 h at 37 °C, were placed in a glass-bottom dish (D35-10-0-N, Cellvis; IBL Baustoff + Labor GmbH, Gerasdorf, Austria) for imaging. These biofilms were imaged using a 60 × water-dipping objective (CFI Plan 60XC W, 2.5 mm working distance, NA 1.0, Nikon Instruments, Amsterdam, the Netherlands). For each porcine valve sample, three z-stacks were captured with a 2 μm step size, producing images of 212 μm × 212 μm at a resolution of 512 × 512 pixels. Time-lapse imaging was performed on *S. aureus* 25268, *S. aureus* 50825, and *S. aureus* 8325-4 grown in human plasma for the first 6 h after inoculation (t = 0) and again at 24 h in Ibidi μ-Slide mono-channels. For these experiments, the confocal microscope was equipped with a 100 × water dipping objective (CFI Plan 100XC W, 2.8 mm working distance, NA 1.1, Nikon Instruments, Amsterdam, the Netherlands). For each time-lapse image, a z-stack of 800 μm was captured at the same location of the slide (from top to bottom) was made with a 2 μm step size at 1–1.9 frames/sec, with each image at 128 μm × 128 μm (with 512 × 512 pixels). To visualize fibrin(ogen) within biofilms, human fibrinogen fluorescently-labeled with Alexa Fluor 647 (final concentration 0.1 mg/ml in plasma containing ~ 2.0 mg/ml; F35200; Thermo Fisher Scientific; excited at 640 nm and detected at 700/75 nm) was added to the plasma just before bacterial inoculation. Before imaging, SYTO™ 9 green fluorescent nucleic acid stain (2 μl/ml; S34854; Thermo Fisher Scientific; excited at 488 nm and detected at 525/50 nm) was used to visualize living bacteria, and propidium iodide (PI; 25 μl/ml; P4864-10 ML; Sigma-Aldrich, Zwijndrecht, the Netherlands; excited at 561 nm and detected at 595/50 nm s), to visualize porcine valvular cells and dead bacteria. Amino sugars (N-Acetylglucosamine) in the biofilms grown on porcine valves were visualized using wheat germ agglutinin (WGA) labeled with Alexa Fluor™ 350 (6 μl/ml W11263; Thermo Fisher Scientific; excited at 405 nm and detected at 425/75 nm).

2.6. Data analysis

Confocal images were obtained and analyzed using Nikon Instruments Software (NIS)-Elements Advanced Research (Version 4.50; Nikon Instruments). Additional post-hoc image analysis on confocal microscopy images was performed using a custom-designed ImageJ/Fiji [27] script (Optical Imaging Center, Erasmus MC, Rotterdam). Briefly, fibrin density was measured by segmenting the fibrin network by thresholding and determining the ratio of density of fibrin over the total imaged volume. The porosity was measured by segmenting the empty spaces inside the fibrin network by thresholding. Subsequently, the largest possible circle centered around the segmented spaces not containing any pixels above an intensity of 1700 was iteratively determined as the threshold. The porosity was calculated by taking the diameter of the fitted circles and calculating the surface. Graphical representation and data analysis (including baseline correction) was performed with Microsoft Excel (Microsoft Corporation, 2010), MATLAB (The MathWorks Inc., Natick, MA, USA, version 2024a), and SPSS (IBM SPSS Statistics, Version 28). Normality of the data was tested using the Shapiro-Wilk test. Statistical significance between groups was determined using Mann-Whitney-U test, and Wilcoxen signed rank test for changes between time points within a group. A p-value <0.05 was considered statistically significant. All quantifiable data points are presented as mean ± standard deviation (SD).

3. Results

3.1. Bacterial growth and metabolic activity is medium and substrate dependent

The effect of different growth media on bacterial growth rates were investigated for *S. aureus* 25268, *S. aureus* Δcoa, and *S. lugdunensis* over a 24 h period. The bacteria were grown in TSB (Fig. 1A; top graph), IMDM (Fig. 1B; middle graph), and human plasma (Fig. 1C; bottom graph). In TSB, *S. aureus* 25268 (blue line) exhibited the highest growth rate and total growth, while *S. aureus* Δcoa (yellow line) and *S. lugdunensis* (green line) showed slower and less growth. In IMDM, *S. aureus* Δcoa and *S. lugdunensis* exhibited delayed growth compared to *S. aureus* 25268. Despite this delay, the final OD values of *S. aureus* Δcoa, *S. lugdunensis* and *S. aureus* 25268 after 24 h were similar. In human plasma, *S. aureus* 25268 had the highest growth rate and final OD, indicating that human plasma was the most favorable medium for its growth. The growth of *S. aureus* Δcoa and *S. lugdunensis* remained lower than that of *S. aureus* 25268 across all three media, except in IMDM after 24 h when all strains reached similar biofilm OD measurements.

The metabolic activity, which includes growth as well as various other processes like virulence factor production (e.g., coagulase), of *S. aureus* 25268, *S. aureus* Δcoa and *S. lugdunensis* was assessed over 24 h in the three different media: TSB (Fig. 2A), IMDM (Fig. 2B) and human plasma (Fig. 2C). Control experiments with sterile TSB, IMDM, and human plasma, both with and without porcine valve biopsies, exhibited no metabolic activity (data not shown). In TSB (Fig. 2A), *S. aureus* 25268 exhibited the highest metabolic activity, peaking at 60.99 ± 1.6 μW (solid blue line). *S. aureus* Δcoa showed a similar peak, albeit lower at 43.8 ± 0.7 μW (solid orange line). *S. lugdunensis* had an even lower metabolic activity, peaking at 17.3 ± 2.4 μW (solid green line). The addition of porcine valve material affected the metabolic activity of all strains differently (Fig. 2A, dashed lines). *S. aureus* 25268 showed reduced activity after 8 h, *S. aureus* Δcoa exhibited increased activity from the time to peak until the 14 h time point before declining, and *S. lugdunensis* had reduced overall activity. The time to reach peak metabolic activity in TSB was approximately 4.5–5 h for the *S. aureus* strains, and 4.5–6.5 h for *S. lugdunensis* (Fig. 3).

In IMDM (Fig. 2B), notable differences were observed compared to TSB for all strains. Without valve tissue, *S. aureus* 25268 peaked around 29.22 ± 5.6 μW, *S. aureus* Δcoa at 21.5 ± 5.4 μW, and *S. lugdunensis* at 12.8 ± 0.7 μW. With porcine valve material, *S. aureus* 25268 took approximately 4 more hours to reach its peak; *S. aureus* Δcoa showed increased activity, peaking higher and lasting again until the 14 h timepoint. It generally took longer to reach peak heat flow in IMDM compared to TSB for all strains, and even later for *S. lugdunensis* on porcine valves which peaked at 17.5 ± 0.8 h (Fig. 3).

In human plasma (Fig. 2C), all strains exhibited the lowest metabolic activity of all three media, with similar heat flow pattern but different maximum heat flows achieved. The addition of porcine valve material again affected heat flow for all strains. For *S. aureus* 25268 in human plasma, it took less time to reach maximum activity without the porcine valve, but for *S. aureus* Δcoa maximum activity was achieved with the valve tissue present (Fig. 3). Overall, bacterial metabolic activity was found to be media- and substrate-dependent. *S. aureus* 25268 demonstrated the highest metabolic activity across all media and the presence of a porcine valve affected the heat flow and time to maximum metabolic activity, and significantly for *S. aureus* 25268 in IMDM and human plasma, and for *S. lugdunensis* in IMDM (Fig. 3).

3.2. Only the coagulase-producing S. aureus strain developed fibrin biofilms

Confocal microscopy was used to visualize fibrin(ogen) presence within biofilms of different strains grown in plasma on porcine valves for 24 h at 37 °C (Fig. 4). Nuclei of porcine valvular cells and dead bacteria,

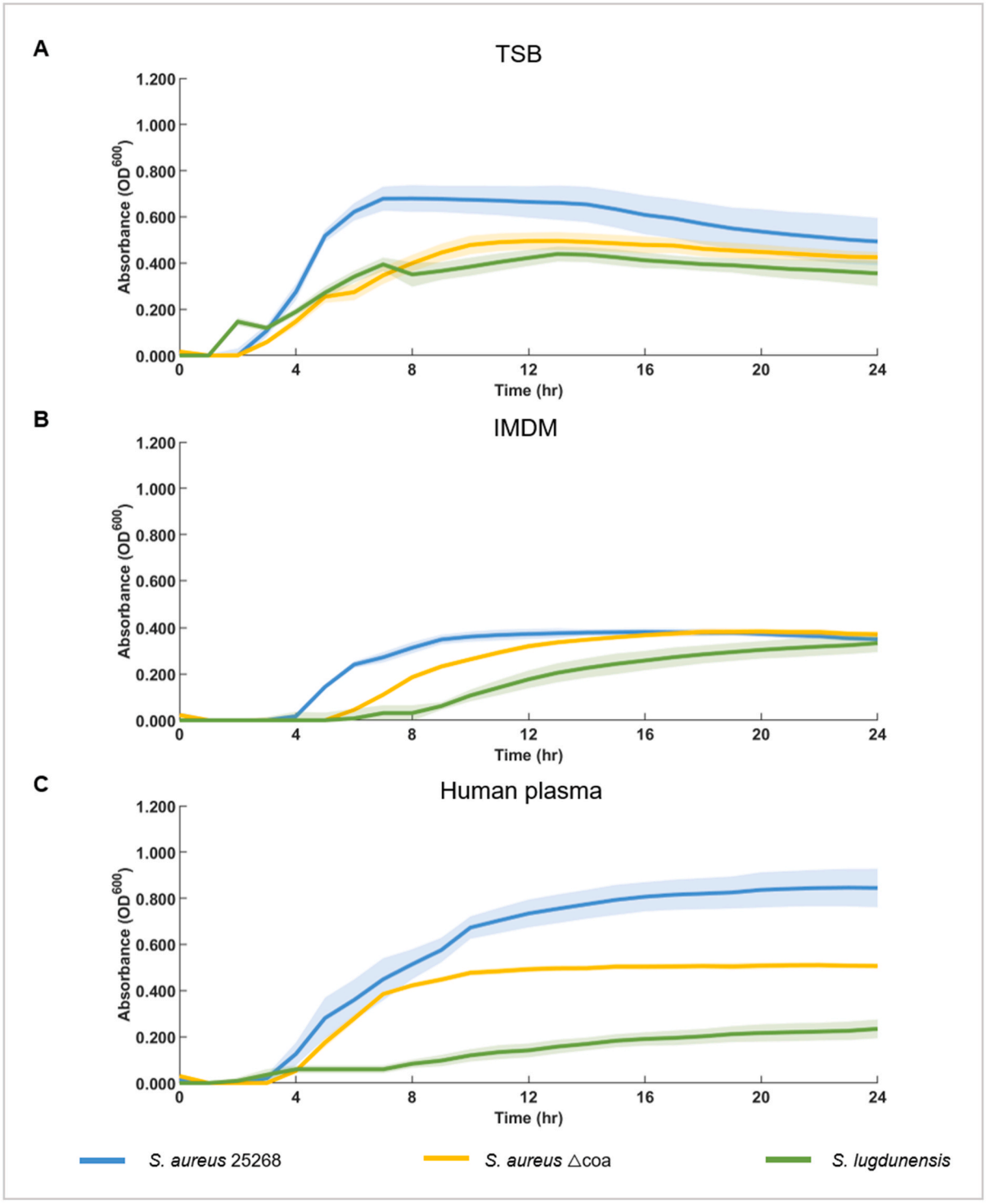

Fig. 1. Bacterial growth curves of three different strains cultured in three different types of growth media. *S. aureus* 25268 (blue), *S. aureus* △coa (yellow), and *S. lugdunensis* (green) were grown in **(A)** tryptic soy broth (TSB), **(B)** Iscove's Modified Dulbecco's Medium (IMDM) and **(C)** human plasma. Bold singular lines represent the mean and the corresponding shadowing represents the standard deviation (n = 4). (For interpretation of the references to color in this figure legend, the reader is referred to the Web version of this article.)

both stained red, could be distinguished based on size difference, as valvular nuclei are oval at ± 10 μm wide and ±4 μm long and dead bacteria are spherical at ± 1 μm in diameter.

Plasma-grown *S. aureus* 25268 developed biofilms with a dense fibrin strand network (pink) covering the surface of the valve (Fig. 4 A1, 2). The majority of the bacteria were living (pseudo colored yellow) and formed aggregates approximately 15–35 μm in size within the fibrin strand network, with fibrin(ogen) found within the aggregates as well as covering the surface. In contrast, *S. aureus* Δcoa (Fig. 4 B1, 2) developed biofilms without any fibrin or fibrinogen and were dispersed over the porcine valve, while it's wild-type strain, *S. aureus* 8325–4 (Fig. S1 A), was able to develop a fibrin network, albeit much less than the clinical *S. aureus* isolates. *S. lugdunensis* (Fig. 4 C1, 2) developed biofilms similar to *S. aureus* Δcoa, without a fibrin network or fibrin strands.

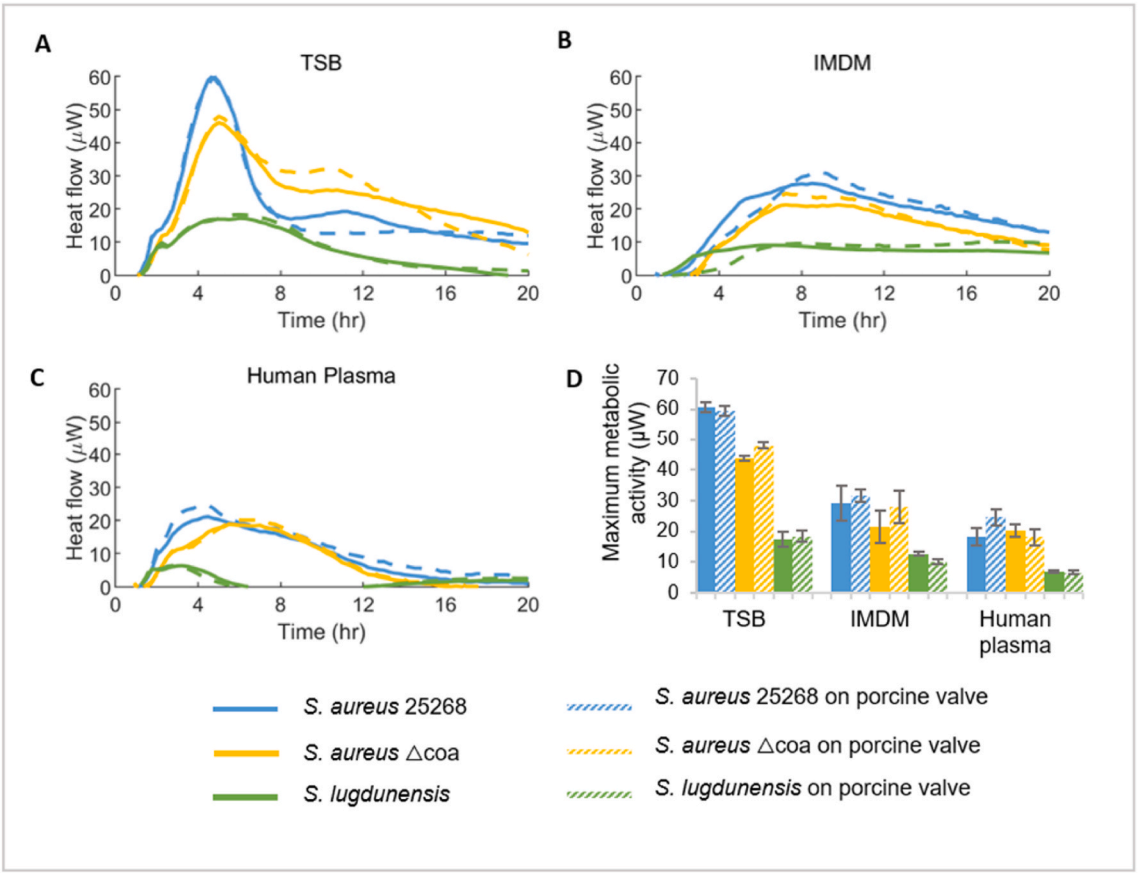

Fig. 2. Total metabolic activity (μW) of **(A)** *S. aureus* 25268, **(B)** *S. aureus* △coa, and **(C)** *S. lugdunensis* measured in tryptic soy broth (TSB), Iscove's Modified Dulbecco's Medium (IMDM), and human plasma with (dashes lines) or without (solid lines) porcine valve biopsies**. (D)** Maximum metabolic activity of each strain. Lines and bars represent the mean. Error bars represent the standard deviation (n = 3).

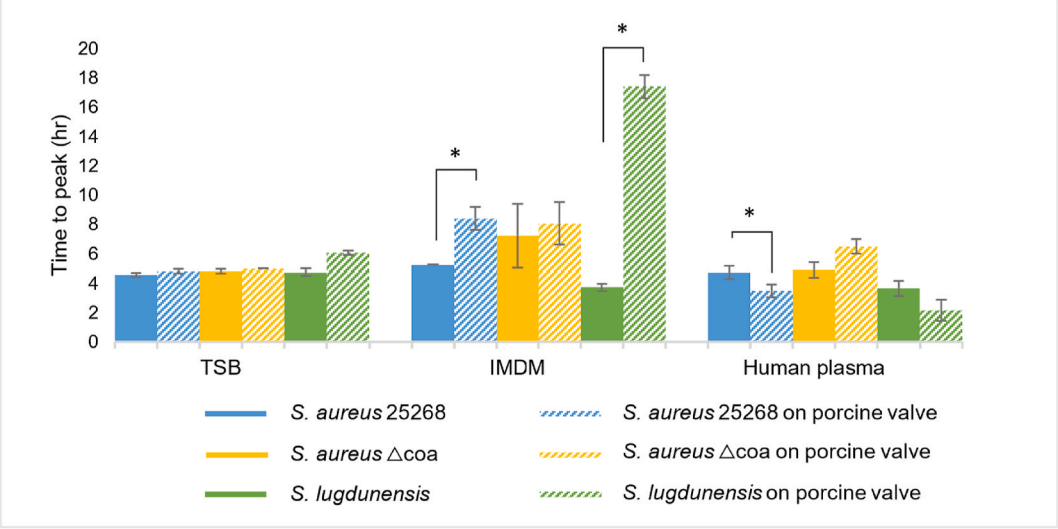

Fig. 3. Time to peak metabolic activity of *S. aureus* 25268, *S. aureus* △coa, and *S. lugdunensis* measured in tryptic soy broth (TSB), Iscove's Modified Dulbecco's Medium (IMDM) and human plasma, with or without porcine valve present. A single asterisk denotes statistical significance ($p < 0.05$), calculated using a Mann-Whitney-U test, between same strains with and without porcine valves. Data is presented as the mean and error bars the standard deviation (n = 3).

3.3. Coagulases are necessary for S. aureus fibrinogen utilization

To further investigate the role of coagulases in the conversion of fibrinogen into fibrin, a fibrinogen utilization assay was performed. Fig. 5 shows the percentage of fibrinogen used by bacteria, i.e., the decrease in fibrinogen measured, during 24 h biofilm development. The starting concentration of fibrinogen in plasma was 2.0 g/l. *S. aureus* 25268 (blue line) showed a rapid increase in fibrinogen utilization, reaching 76.4 % within 6 h, 78.1 % at 9 h, and then maintaining this level for the duration of the 24 h period. *S. aureus* Δcoa (yellow line)

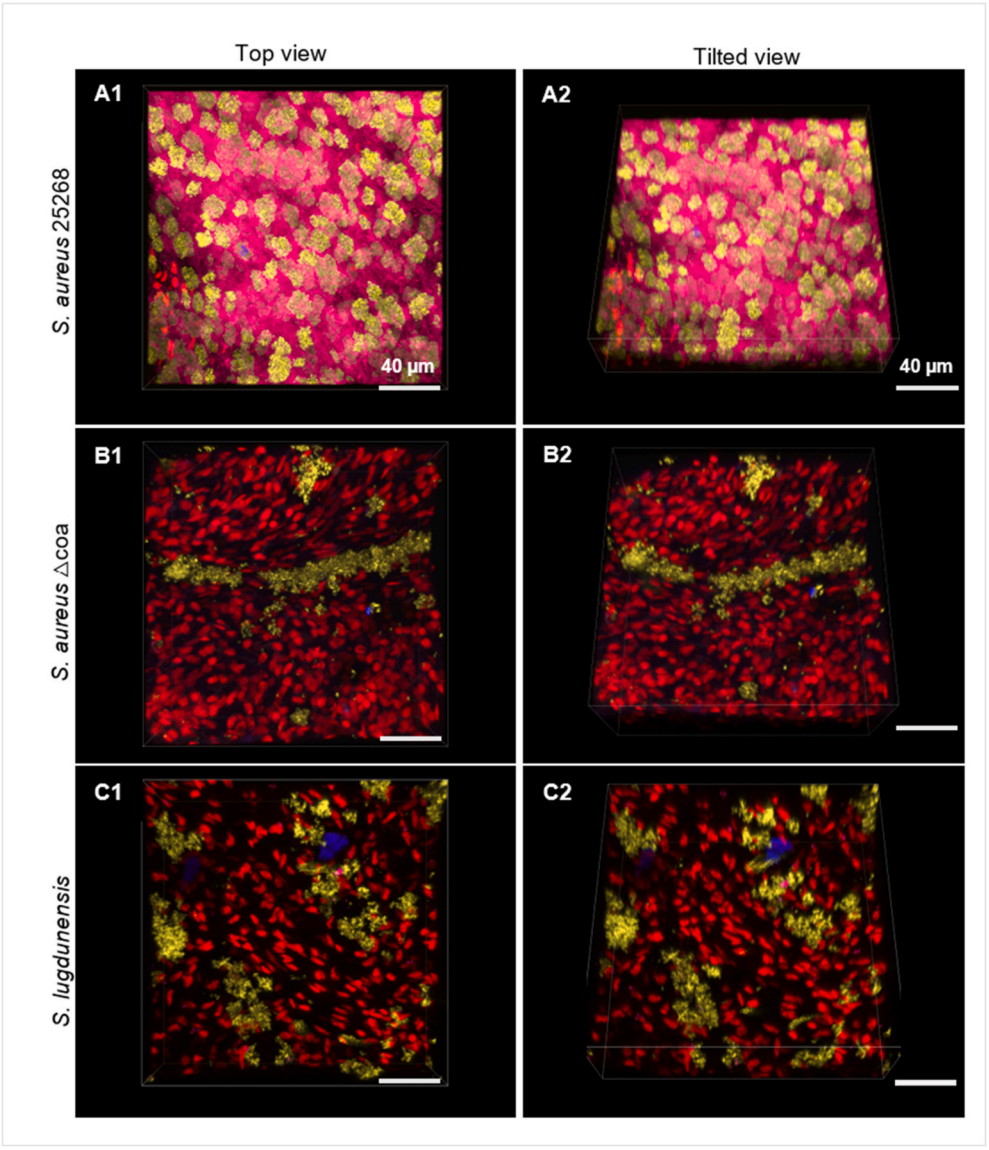

Fig. 4. Confocal three-dimensional volume-rendered images of *S. aureus* 25268 (**A**), *S. aureus* △coa (**B**), and *S. lugdunensis* (**C**) biofilms grown for 24 h at 37 °C in human plasma on porcine valves. **A1**, **B1**, **C1** are the top views of biofilms, while **A2, B2, C3** are corresponding views at an angle. For all images, blue (Alexa Fluor 350 wheat germ agglutinin) indicates amino sugars, yellow (pseudo-colored; Syto9) indicates living bacteria, red (propidium iodide) indicates valvular cells and dead bacteria, and pink (Alexa Fluor 647) indicates fibrin and fibrinogen. All images are representative of three separate experiments. (For interpretation of the references to color in this figure legend, the reader is referred to the Web version of this article.)

exhibited minimal fibrinogen utilization, with only 5.1 % maximally measured over 24 h, which was consistent with the plasma-only control samples (red line). *S. lugdunensis* (green line) showed a similar fibrinogen utilization of 5.9 % after 24 h. While *S. aureus* 8325–4 (purple line) reached 9.0 % at 24 h (Fig. S1 B). A significant drop in fibrinogen levels was observed for *S. aureus* 25268 between 2 and 6 h, 74.9 % ($p = 0.034$), indicating a sharp increase in fibrinogen utilization during this period. This was not observed in the coagulase-negative strains, *S. aureus* Δcoa and *S. lugdunensis* or in the plasma-only control samples.

3.4. Fibrin network development occurs within the first 6 h

The development of the fibrin network in biofilms formed by different strains of *S. aureus* were analyzed using time-lapse imaging. Fig. 6 provides representative images of fibrin network development for *S. aureus* 25268 (Fig. 6A) and *S. aureus* 50825 (Fig. 6B). In each image, fibrin(ogen) (pink) was fluorescently-labeled to visualize the biofilm structure. Early time points (1–3 h) revealed sparse and scattered bacterial cells covered in fibrin(ogen), while later time points (4–6 h) quickly showed a progressive increase in density of fibrin strands and growing aggregates of bacteria within the biofilm matrix. *S. aureus* 25268 was observed to form denser fibrin biofilms faster than *S. aureus* 50825. The appearance of initial fibrin strands, assessed visually, was at 1.8 ± 0.3 h for *S. aureus* 25268 and 2.0 ± 0.0 h for *S. aureus* 50825. By 24 h, biofilms reached a mature state for both strains, as indicated by the dense and confluent matrix observed. *S. aureus* 8325-4 developed a fibrin network around the bacterial colonies (Figure S1C), however this formed much later and less dense then the clinical *S. aureus* strains, supporting the fibrinogen utilization data. The tracking fibrin network development showed that fibrin strands did not originate from the bacterial aggregates, but first formed within the plasma appearing to freely move about and then subsequently attach to the aggregates and other fibrin strands (Video 1).

Supplementary data related to this article can be found online at https://doi.org/10.1016/j.bioflm.2025.100261

Further analysis of the fibrin network was performed on the images

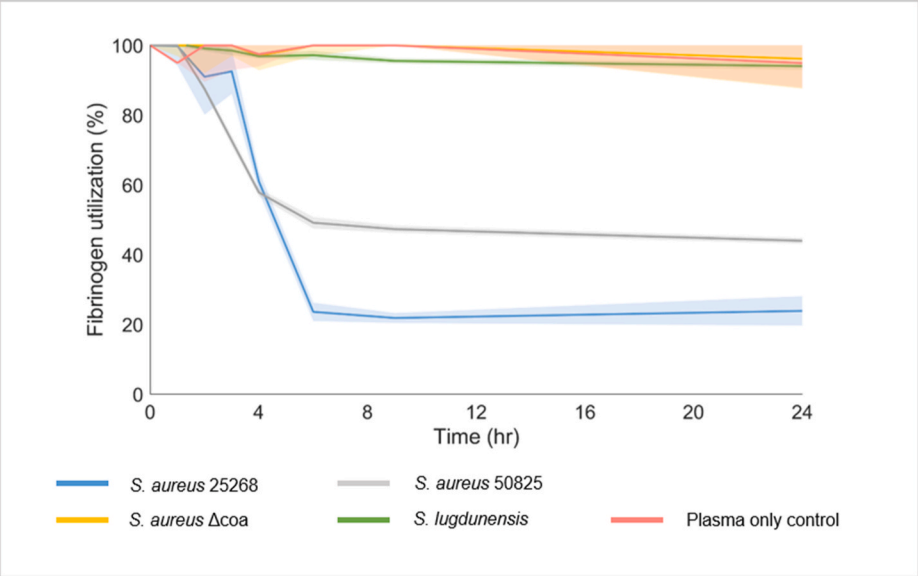

Fig. 5. Bacterial fibrinogen utilization of *S. aureus* 25268 (blue), *S. aureus* △coa (yellow) and *S. lugdunensis* (green) over 24 h. Human plasma alone (red) was used as a control. Solid lines represent the mean and shading the standard deviation of three independent experiments. (For interpretation of the references to color in this figure legend, the reader is referred to the Web version of this article.)

to assess the porosity (Fig. 7A; top graph), and fibrin density (Fig. 7B; bottom graph) of the biofilms over time. Initially, the porosity is high but decreases as the biofilm matures, indicating a denser fibrin biofilm architecture with less free space. *S. aureus* 50825 showed an 82.1 ± 9.0 % decrease ($p = 0.413$) in porosity between 6 and 24 h, whereas *S. aureus* 25268 showed a 29.7 ± 4.4 % decrease ($p = 0.003$). Despite the variations in porosity between strains, the final porosity of the fibrin network developed by both strains after 24 h was similar (11.78 % difference). The total fibrin(ogen) density in the biofilms (Fig. 7B) increased over time, with a noticeable difference between the two strains. *S. aureus* 25268 produced a more rapid and higher increase in biofilm density compared to *S. aureus* 50825, suggesting strain-specific differences in biofilm formation capabilities. Between 2 and 6 h, *S. aureus* 25268 showed a 15.0 ± 7.5-fold increase ($p = 0.043$) in fibrin (ogen) density, and *S. aureus* 50825 showed a 12.2 ± 4.2-fold increase ($p = 0.006$). This outcome is consistent with the bacterial utilization of fibrinogen, where a significant decrease in fibrinogen levels was found between 2 and 6 h of biofilm development.

4. Discussion

In this study, we found that bacteria behaved differently depending on the culture medium and substrate, i.e., whether it grew on porcine valve tissue or hard surface, highlighting the importance experimental design. Only coagulase-producing *S. aureus* isolates formed fibrin biofilms by converting fibrinogen. Furthermore, quantification of the fibrin density and porosity showed strain-dependent fibrin network development over time. These results provide important insights into the significance of coagulase as key mediator of fibrin development in biofilms.

Both bacterial growth and metabolic activity were found to be medium-dependent. For *S. aureus* 25268, maximum metabolic activity was higher in TSB; however, the highest OD was measured in plasma after 24 h, suggesting a dense biofilm was produced in plasma even though the bacteria were less metabolically active. This difference in maximum metabolic rate can be attributed to the bacterial-specific high nutrient content of TSB, especially its higher glucose levels compared to plasma (2.5 g/l in TSB versus 1.0–1.4 g/l in human plasma) [28,29]. The higher OD in human plasma can be explained by the formation of a dense fibrin biofilm by *S. aureus* (Fig. 4), which is not possible in TSB. Bacterial growth of the coagulase-negative strains was similar across all three media, however their time to reach maximum OD differed with each media. Larger differences were found when comparing to metabolic activity. While metabolic activity is a proxy for bacterial growth, it is not synonymous; metabolic activity can also refer to other bacterial activities, such as virulence factor production, indicating that the bacteria are alive and active [30]. Substrate-dependent alterations in metabolic activity were also observed between bacteria growing on heart valve tissue (to mimic infective endocarditis) or a hard surface (to mimic a cardiovascular device infection) (Figs. 2 and 3), suggesting that the same bacterial strain behaves differently depending on whether it grows on tissue or a device. For example, the tissue surface increased bacterial activity for *S. aureus* 25268 in plasma, and for *S. lugdunensis* the similar peak metabolic activity was on a hard surface and heart valve tissue, while the time to reach peak metabolic activity was significantly delayed when grown on a porcine valve. Overall, these findings underscore the importance of substrate and medium choice to best match the research study goals, such as the development of soft-tissue infections versus device-related infections and where within or on the human body.

Several *in vitro* and *ex vivo* models have been used to investigate *S. aureus* fibrin biofilm formation [18,19,21] such as the classical static biofilm assay [31,32] and wound infection models [33–35], however, not using 100 % human plasma as a growth medium. Models using human plasma provide a more realistic mimic of *in vivo* cardiovascular biofilms compared to traditional growth (e.g., TSB, BHI) or mammalian cell culture media (e.g., RPMI, IMDM), as highlighted by our findings on bacterial responses to different media (Figs. 1–3). Coating surfaces and supplementing media with human plasma had been shown to influence biofilm formation and facilitate bacterial attachment [18,19,21,36]. It has also been shown that expression of microbial surface components recognizing adhesive matrix molecules (MSCRAMMs), which are surface proteins bacterial adhesins expressed by *S. aureus* that are essential for initial bacterial attachment, are upregulated in MHB when supplemented with human plasma [19]. We found that coagulase production is crucial for fibrin network formation in *S. aureus* biofilms in human plasma. This finding aligns with prior research highlighting the significance of coagulase enzymes produced by *S. aureus* [21,37]. Trivedi et al. (2018) studied the role of both coagulases, staphylocoagulase and von Willebrand factor binding protein, by comparing clot generation between coagulase mutant strains [37]. They found that staphylocoagulase

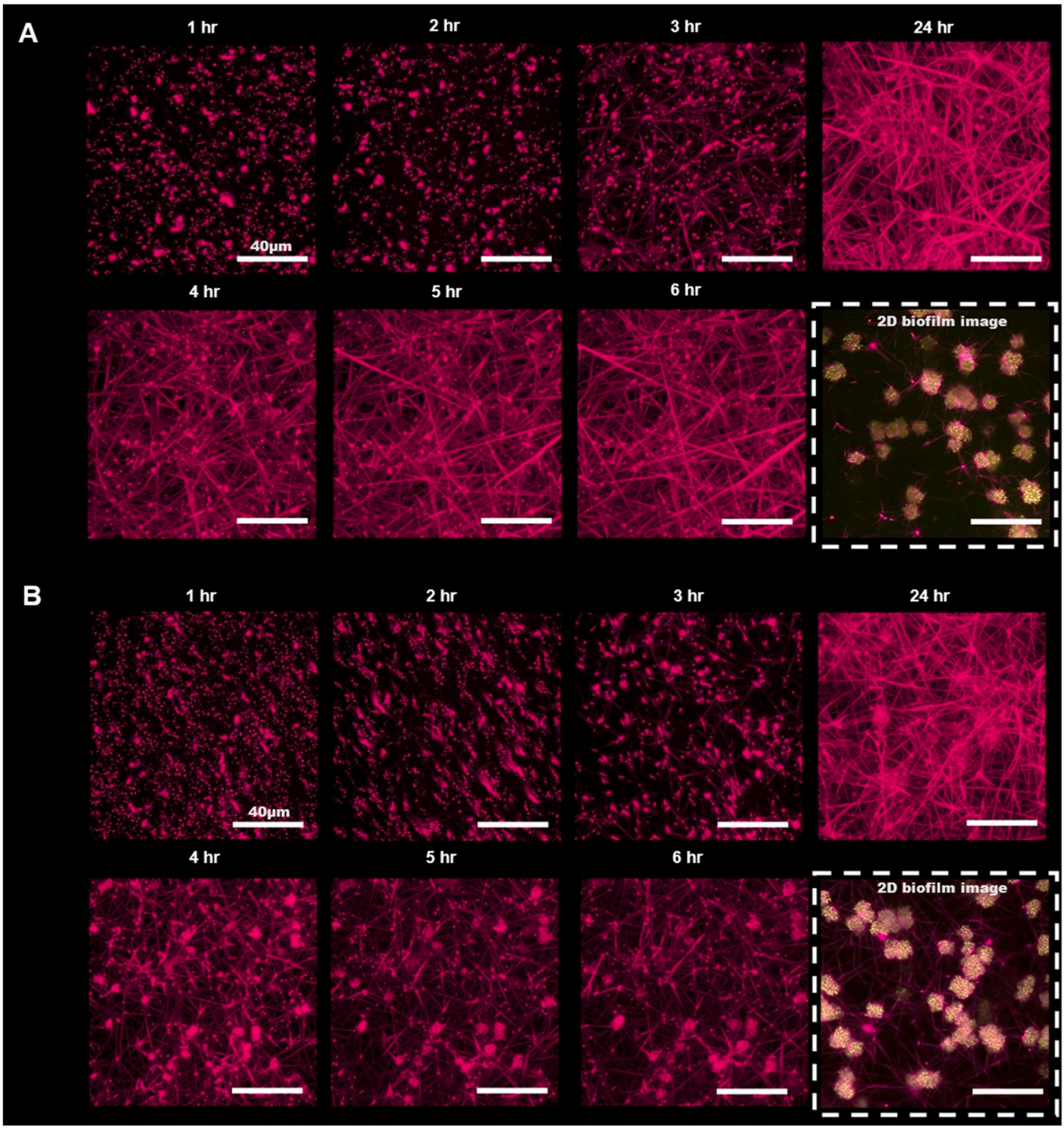

Fig. 6. Fibrin network development over time. (**A**, **B**) Three-dimensional volume rendering confocal microscopy of fibrin(ogen) (pink; Alexa Fluor 647) at 1, 2, 3, 4, 5, 6 and 24 h for two plasma-grown strains, **(A)** *S. aureus* 25268 and **(B)** *S. aureus* 50825. At 24 h, bacteria were also fluorescently-labeled (yellow; Syto9) to visualize the bacteria within the developed fibrin network, shown as a 2D image (dashed white border). All images are representative of three independent experiments for each strain. (For interpretation of the references to color in this figure legend, the reader is referred to the Web version of this article.)

mutant strains unable to produce staphylocoagulase could not induce clot formation in a wound like model while a von Willebrand factor binding protein (vWbp) mutant strain could still induce clot formation after 24 h incubation [37]. Similarly, Zapatozcoa et al. (2015) showed that, on plasma-coated surfaces, a vWbp mutation had no significant effect on biofilm development in RPMI medium [21]. The importance of staphylocoagulase has also been demonstrated *in vivo*. Using a rat model, Lerche et al. (2019) showed that adjunctive dabigatran therapy improves outcomes in left-sided S. aureus IE, emphasizing the potential of targeting coagulase activity [38] and Veloso et al. (2015) showed prophylactic use of antiplatelet and antithrombin agents are effective for the long-term prevention of IE [39]. These findings highlight the critical role of coagulation pathways in both the pathogenesis and therapeutic management of S. aureus IE.

In our study, confocal microscopy imaging of the biofilms after 24 h revealed fibrin-encased bacterial aggregates in coagulase-positive

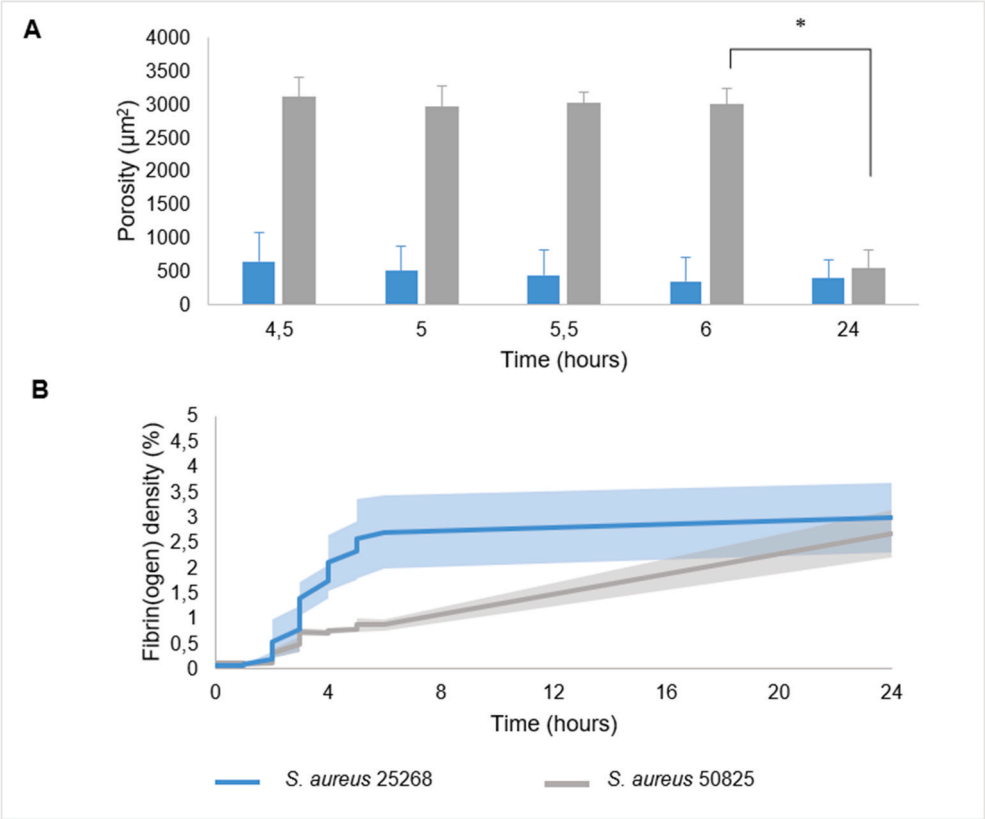

Fig. 7. Quantification of the porosity (**A**) and total fibrin(ogen) density (**B**) of the fibrin networks in 3D volume rendering time-lapse confocal microscopy (examples in Fig. 6) of plasma grown *S. aureus* 25268 (blue) and *S. aureus* 50825 (grey). A single asterisk denotes statistical significance ($p < 0.05$), calculated using a Wilcoxen signed rank test, between two time points. Solid lines represent the mean and shading the standard deviation of three independent experiments. (For interpretation of the references to color in this figure legend, the reader is referred to the Web version of this article.)

S. aureus strains grown in human plasma (Fig. 4). In contrast, coagulase-negative strains showed bacteria on the porcine valves without fibrin. For coagulase-positive *S. aureus* strains, the presence of fibrin provides a physical scaffold for bacterial cells [40], influencing cell-to-cell interactions and promoting the aggregation of cells within the biofilm matrix [41], while other factors, such as complement activation [42], may contribute to the pathogenesis of coagulase-negative strains.

Further investigation into the fibrin network development revealed that the volume of fibrin increases exponentially within the first 6 h of biofilm development (Fig. 6). During this period, fibrinogen utilization by the *S. aureus* 25268 strain increased exponentially (Fig. 5). The decrease in fibrinogen levels in the plasma over time reflects the binding of fibrinogen to the bacteria themselves or conversion into fibrin used to form the biofilms. This finding aligns with a previous study by Rogers (1954), which showed that the coagulase concentration, measured by clotting time in whole human plasma, in culture supernatant increased exponentially within the first 6 h of development and ceased earlier than bacterial growth [43]. This suggests that coagulases are used primarily during the initial development of the biofilm to form a fibrin biofilm, especially since not all of the fibrinogen in the plasma was utilized (Fig. 5). Distinct variations in porosity and volume of the developed fibrin networks were observed between *S. aureus* strains (Fig. 7). These differences in the fibrin network development could have significant implications for disease progression. One possibility is that the different amount of activity or rate of coagulase produced by *S. aureus* may lead to modifications in the fibrinogen-to-fibrin conversion process, thereby affecting the structural integrity and organization of the resulting fibrin network. These differences may have an impact on disease severity, as Cheng et al. (2010) previously found that time to death in mice was significantly delayed when infections were induced using a coagulase negative mutant *S. aureus* strain instead of a coagulase positive *S. aureus* strain [44].

Human plasma is a better mimic of *in vivo* cardiovascular biofilm development than TSB or IMDM. The human plasma used in our study was not heat-inactivated to preserve functional integrity of plasma proteins, meaning that donor-specific antibodies against *S. aureus* may have been present. To ensure consistency and minimize variability between outcomes, pooled human plasma from five healthy donors was used for all experiments. The plasma was anticoagulated using citrate phosphate double dextrose (CP2D), a well-established and FDA-approved method (FDA, Citrate Phosphate Dextrose Anticoagulant Solution). CP2D chelates calcium ions, preventing clot formation and reducing platelet reactivity, thereby maintaining the plasma in an anticoagulated state and ensuring controlled re-coagulation. The choice of substrate for an *in vitro* model should also be carefully selected based on the specific research goal. For instance, Sunnerhagen et al. (2024) used prosthetic valve material to study bacterial adhesion to aortic valve implants [45], and Schwartz et al. (2021) developed a human *in vitro* vegetation simulation model using a leucocyte- and platelet-rich fibrin patch to test antibiotic efficacy on biofilms [46]. Our model focuses capturing the early stages of fibrin biofilm development under physiological conditions relevant to cardiovascular infections. In our current model, several factors in the human body, such as immune and red blood cells, are not present. For instance, fibrin formation can trigger immune activation and subsequent recruitment of inflammatory cells, such as neutrophils, to the infection site, which may influence biofilm development [47]. Moreover, platelets have been shown to contribute to the pathogenesis of *S. aureus* infections by promoting bacterial adhesion and biofilm formation [48]. Despite these limitations, our current model provides a good basis for building increasingly complex models that, for

instance, incorporate shear flow and for performing intervention experiments. Future studies should consider expanding the complexity to further include whole blood components in order to understand how these factors also effect early fibrin biofilm development. A limitation of this study is the detection limit of 0.4 g/l of fibrinogen in the Sysmex CS-5100 system.

In conclusion, this study highlights the critical role of coagulases in the formation of fibrin biofilms by *S. aureus*. Our findings reveal significant differences in fibrin network development, porosity, and volume between coagulase-positive and coagulase-negative strains, emphasizing the complex interplay between bacterial metabolism and biofilm architecture. The ability of *S. aureus* to utilize fibrinogen and form dense biofilms in human plasma demonstrates the importance of coagulase as a key mediator in the pathogenesis of cardiovascular infections. These insights provide support for novel therapeutic approaches targeting coagulase activity to potentially disrupt biofilm formation and mitigate infection severity [49,50]. Furthermore, this study showed that the media and even the substrate bacteria grow on influence bacterial activity, emphasizing the need for advanced *in vitro* models that incorporate total human blood components and *in vivo* found substrates. Future research with a focus on understanding the specific mechanisms underlying differences in fibrin network development can provide insights into the pathogenesis of *S. aureus* infections. By advancing our understanding of these critical processes, we can develop more effective strategies to address life-threatening fibrin biofilm-associated infections.

CRediT authorship contribution statement

Safae Oukrich: Writing – review & editing, Writing – original draft, Visualization, Validation, Project administration, Methodology, Investigation, Formal analysis, Data curation, Conceptualization. **Jane Hong:** Writing – review & editing, Data curation. **Mariël Leon-Grooters:** Writing – review & editing. **Wiggert A. van Cappellen:** Writing – review & editing, Software. **Johan A. Slotman:** Writing – review & editing, Software. **Gijsje H. Koenderink:** Writing – review & editing, Methodology. **Willem J.B. van Wamel:** Writing – review & editing, Validation, Resources, Methodology. **Moniek P.M. de Maat:** Writing – review & editing, Validation, Resources, Methodology. **Klazina Kooiman:** Writing – review & editing, Validation, Supervision, Resources, Methodology, Funding acquisition. **Kirby R. Lattwein:** Writing – review & editing, Writing – original draft, Validation, Resources, Methodology, Data curation, Conceptualization.

Institutional review board statement

Ethical review and approval were waived for this study due to anonymization and de-identification of the bacterial isolates, according to institutional policy.

Funding

This work was supported by the Dutch Heart Foundation, Dekkerbeurs grant number 03-006-2023-0088, awarded to K.L. and the European Research Council (ERC) under the European Union's Horizon 2020 research and innovation program, grant number 805308, awarded to K. K.

Declaration of competing interests

The authors declare no conflict of interests.

Acknowledgments

The authors would like to thank Debby Priem, Iris van Moort, and other members of the Hemostasis Laboratory from the Department of Hematology at Erasmus MC, Rotterdam, the Netherlands, for their skillful assistance with the fibrinogen utilization determination. The authors also thank the members of the Therapeutic Ultrasound Contrast Agent group (Biomedical Engineering, Dept. of Cardiology) and the *S. aureus* working group (Dept. of Medical Microbiology and Infectious Diseases) at the Erasmus MC, Rotterdam, the Netherlands for their input, help, and useful discussions.

Appendix A. Supplementary data

Supplementary data to this article can be found online at https://doi.org/10.1016/j.bioflm.2025.100261.

Data availability

Data will be made available on request.

References

[1] Kouijzer JJP, et al. Native valve, prosthetic valve, and cardiac device-related infective endocarditis: a review and update on current innovative diagnostic and therapeutic strategies. Front Cell Dev Biol 2022;10.
[2] Sandoe JA, et al. New guidelines for prevention and management of implantable cardiac electronic device-related infection. Lancet 2015;385(9984):2225–6.
[3] El Kadi S, et al. Infective endocarditis in The Netherlands: current epidemiological profile and mortality : an analysis based on partial ESC EORP collected data. Neth Heart J 2020;28(10):526–36.
[4] Lalani T, et al. In-hospital and 1-year mortality in patients undergoing early surgery for prosthetic valve endocarditis. JAMA Intern Med 2013;173(16):1495–504.
[5] Thyagarajan B, et al. Endocarditis in left ventricular assist device. Intractable Rare Dis Res 2016;5(3):177–84.
[6] Liesenborghs L, et al. Coagulation: at the heart of infective endocarditis. J Thromb Haemostasis 2020;18(5):995–1008.
[7] Tong SY, et al. Staphylococcus aureus infections: epidemiology, pathophysiology, clinical manifestations, and management. Clin Microbiol Rev 2015;28(3):603–61.
[8] Das AS, et al. Risk factors for neurological complications in left-sided infective endocarditis. J Neurol Sci 2022;442:120386.
[9] Slipczuk L, et al. Infective endocarditis epidemiology over five decades: a systematic review. PLoS One 2013;8(12):e82665.
[10] Mah TF, O'Toole GA. Mechanisms of biofilm resistance to antimicrobial agents. Trends Microbiol 2001;9(1):34–9.
[11] Kwiecinski J, et al. Staphylokinase control of Staphylococcus aureus biofilm formation and detachment through host plasminogen activation. J Infect Dis 2016;213(1):139–48.
[12] Cahill TJ, Prendergast BD. Infective endocarditis. Lancet 2016;387(10021):882–93.
[13] Antoniak S. The coagulation system in host defense. Res Pract Thromb Haemost 2018;2(3):549–57.
[14] Flores-Mireles AL, et al. EbpA vaccine antibodies block binding of Enterococcus faecalis to fibrinogen to prevent catheter-associated bladder infection in mice. Sci Transl Med 2014;6(254):254ra127.
[15] Sillanpää J, et al. A family of fibrinogen-binding MSCRAMMs from Enterococcus faecalis. Microbiology (Read) 2009;155(Pt 7):2390–400.
[16] Whitnack E, Beachey EH. Biochemical and biological properties of the binding of human fibrinogen to M protein in group A streptococci. J Bacteriol 1985;164(1):350–8.
[17] Zapotoczna M, O'Neill E, O'Gara JP. Untangling the diverse and redundant mechanisms of Staphylococcus aureus biofilm formation. PLoS Pathog 2016;12(7):e1005671.
[18] Jørgensen NP, et al. Streptokinase treatment reverses biofilm-associated antibiotic resistance in Staphylococcus aureus. Microorganisms 2016;4(3).
[19] Cardile AP, et al. Human plasma enhances the expression of Staphylococcal microbial surface components recognizing adhesive matrix molecules promoting biofilm formation and increases antimicrobial tolerance in Vitro. BMC Res Notes 2014;7:457.
[20] Scull G, et al. Fighting fibrin with fibrin: vancomycin delivery into coagulase-mediated Staphylococcus aureus biofilms via fibrin-based nanoparticle binding. J Biomed Mater Res 2024;112(12):2071–85.
[21] Zapotoczna M, et al. An essential role for coagulase in Staphylococcus aureus biofilm development reveals new therapeutic possibilities for device-related infections. J Infect Dis 2015;212(12):1883–93.
[22] Dietrich M, Besser M, Stuermer EK. Characterization of the human plasma biofilm model (hpBIOM) to identify potential therapeutic targets for wound management of chronic infections. Microorganisms 2024;12(2).
[23] Besser M, et al. Impact of probiotics on pathogen survival in an innovative human plasma biofilm model (hpBIOM). J Transl Med 2019;17(1):243.
[24] Lattwein KR, et al. An in vitro proof-of-principle study of sonobactericide. Sci Rep 2018;8(1):3411.

[25] Clauss A. [Rapid physiological coagulation method in determination of fibrinogen]. Acta Haematol 1957;17(4):237–46.
[26] Beekers I, et al. Combined confocal microscope and brandaris 128 ultra-high-speed camera. Ultrasound Med Biol 2019;45(9):2575–82.
[27] Schindelin J, et al. Fiji: an open-source platform for biological-image analysis. Nat Methods 2012;9(7):676–82.
[28] Lade H, et al. Biofilm Formation by Staphylococcus aureus clinical isolates is differentially affected by glucose and sodium chloride supplemented culture media. J Clin Med 2019;8(11).
[29] Gurung PZM, Jialal I. Plasma glucose. Treasure Island (FL): StatPearls Publishing; Jan 2024. StatPearls [Internet].
[30] Rudra P, Boyd JM. Metabolic control of virulence factor production in Staphylococcus aureus. Curr Opin Microbiol 2020;55:81–7.
[31] Gries CM, et al. Staphylococcus aureus fibronectin binding protein A mediates biofilm development and infection. Infect Immun 2020;88(5).
[32] Sultan AR, et al. Production of staphylococcal complement inhibitor (SCIN) and other immune modulators during the early stages of Staphylococcus aureus biofilm formation in a mammalian cell culture medium. Infect Immun 2018;86(8).
[33] Cheng Y, De Bank PA, Bolhuis A. An in vitro and ex vivo wound infection model to test topical and systemic treatment with antibiotics. J Appl Microbiol 2022;133(5):2993–3006.
[34] Haisma EM, et al. Inflammatory and antimicrobial responses to methicillin-resistant Staphylococcus aureus in an in vitro wound infection model. PLoS One 2013;8(12):e82800.
[35] Steinstraesser L, et al. A novel human skin chamber model to study wound infection ex vivo. Arch Dermatol Res 2010;302(5):357–65.
[36] Cardoso Guimarães L, et al. Increased biofilm formation by Staphylococcus aureus clinical isolates on surfaces covered with plasma proteins. J Med Microbiol 2021;70(8).
[37] Trivedi U, et al. Staphylococcus aureus coagulases are exploitable yet stable public goods in clinically relevant conditions. Proc Natl Acad Sci USA 2018;115(50):E11771–9.
[38] Lerche CJ, et al. Adjunctive dabigatran therapy improves outcome of experimental left-sided Staphylococcus aureus endocarditis. PLoS One 2019;14(4):e0215333.
[39] Veloso TR, et al. Prophylaxis of experimental endocarditis with antiplatelet and antithrombin agents: a role for long-term prevention of infective endocarditis in humans? J Infect Dis 2015;211(1):72–9.
[40] Kwiecinski J, et al. Tissue plasminogen activator coating on implant surfaces reduces Staphylococcus aureus biofilm formation. Appl Environ Microbiol 2016;82(1):394–401.
[41] Kwiecinski J, Jin T, Josefsson E. Surface proteins of Staphylococcus aureus play an important role in experimental skin infection. Apmis 2014;122(12):1240–50.
[42] Otto M. Staphylococcus epidermidis–the 'accidental' pathogen. Nat Rev Microbiol 2009;7(8):555–67.
[43] Rogers HJ. The rate of formation of hyaluronidase, coagulase and total extracellular protein by strains of Staphylococcus aureus. J Gen Microbiol 1954;10(2):209–20.
[44] Cheng AG, et al. Contribution of coagulases towards Staphylococcus aureus disease and protective immunity. PLoS Pathog 2010;6(8):e1001036.
[45] Sunnerhagen T, et al. Transcatheter aortic valve implantation (TAVI) prostheses in vitro - biofilm formation and antibiotic effects. Biofilms 2024;8:100236.
[46] Schwartz FA, et al. Novel human in vitro vegetation simulation model for infective endocarditis. Apmis 2021;129(11):653–62.
[47] Costantini TW, et al. The intersection of coagulation activation and inflammation after injury: what you need to know. J Trauma Acute Care Surg 2024;96(3):347–56.
[48] Vaudaux P, et al. Host factors selectively increase staphylococcal adherence on inserted catheters: a role for fibronectin and fibrinogen or fibrin. J Infect Dis 1989;160(5):865–75.
[49] McAdow M, et al. Preventing Staphylococcus aureus sepsis through the inhibition of its agglutination in blood. PLoS Pathog 2011;7(10):e1002307.
[50] Vanassche T, et al. Dabigatran inhibits Staphylococcus aureus coagulase activity. J Clin Microbiol 2010;48(11):4248–50.